Sensorimotor Cortex Localization: Comparison of Magnetoencephalography, Functional MR Imaging, and Intraoperative Cortical Mapping[1]

Antti Korvenoja, MD
Erika Kirveskari, MD, PhD
Hannu J. Aronen, MD, PhD
Sari Avikainen, MD, PhD
Antti Brander, MD, PhD
Juha Huttunen, MD, PhD
Risto J. Ilmoniemi, PhD
Juha E. Jääskeläinen, MD, PhD
Tero Kovala, MD, PhD
Jyrki P. Mäkelä, MD, PhD
Eero Salli, PhD
Mika Seppä, MSc

Purpose: To prospectively evaluate magnetoencephalography (MEG) and functional magnetic resonance (MR) imaging, as compared with intraoperative cortical mapping, for identification of the central sulcus.

Materials and Methods: Fifteen patients (six men, nine women; age range, 25–58 years) with a lesion near the primary sensorimotor cortex (13 gliomas, one cavernous hemangioma, and one meningioma) were examined after institutional review board approval and written informed consent from each patient were obtained. At MEG, evoked magnetic fields to median nerve stimulation were recorded; at functional MR imaging, hemodynamic responses to self-paced palmar flexion of the wrist were imaged. General linear model analysis with contextual clustering ($P < .01$) was used to analyze functional MR imaging data, and dipole modeling was used to analyze MEG data. MEG and functional MR localizations were compared with intraoperative cortical mappings. The distance from the area of functional MR imaging activation to the tumor margin was compared between the patients with discordant and those with concordant intraoperative mapping findings by using unpaired *t* testing.

Results: MEG depicted the central sulcus correctly in all 15 patients, as verified at intraoperative mapping. The functional MR imaging localization results agreed with the intraoperative mappings in 11 patients. In all four patients with a false localization, the primary activation was in the postcentral sulcus region, but it did not differ significantly from the primary activation in the patients with correct localization with respect to proximity to the tumor ($P = .38$). Furthermore, at functional MR imaging, multiple nonprimary areas were activated, with considerable interindividual variation.

Conclusion: Although both MEG and functional MR imaging can provide useful information for neurosurgical planning, in the present study, MEG proved to be superior for locating the central sulcus. Activation of multiple nonprimary cerebral areas may confound the interpretation of functional MR imaging results.

[1] From the Functional Brain Imaging Unit, Helsinki Brain Research Center, Medical Imaging Center, University of Helsinki, Helsinki, Finland (A.K., H.J.A., E.S.); Brain Research Unit, Low Temperature Laboratory, Helsinki University of Technology, Espoo, Finland (E.K., S.A., J.P.M., M.S.); BioMag Laboratory, Helsinki Brain Research Center, Engineering Centre (A.K., R.J.I.) and Department of Clinical Neurophysiology (E.K., J.H., T.K.), Helsinki University Central Hospital, Helsinki, Finland; Department of Neurosurgery, Kuopio University Hospital, Kuopio, Finland (J.E.J.); and Department of Radiology, Hyvinkää Hospital, Hospital District of Helsinki and Uusimaa, Hyvinkää, Finland (A.B.). From the 2000 RSNA Annual Meeting. Received May 10, 2005; revision requested July 8; revision received September 8; accepted October 14; final version accepted November 23. Supported by grants from the Finnish Radiological Society, Maire Taponen Foundation, Maud Kuistila Foundation, Finnish Cancer Organization, Helsinki University Central Hospital, Academy of Finland, Nordic Cancer Union, Sigrid Juselius Foundation, and Helsinki University Hospital Clinical Research Institute. **Address correspondence to** A.K., Radiology Department, Biomedicum Helsinki, PO Box 700, FI-00029 HUS, Helsinki, Finland (e-mail: *antti.korvenoja@helsinki.fi*).

Neurosurgical procedures are associated with a risk of dysfunction because they can cause damage to functionally important structures adjacent to the areas targeted for surgery. Defining the cerebral functional anatomy on the basis of anatomic landmarks can be unreliable (1,2)—for example, because cerebral lesions may distort the local anatomy of the brain. Furthermore, an expansive lesion may lead to functional reorganization and alter the topographic organization of the cortex (3,4). Therefore, characterization of the functional anatomy in the region of interest in candidates for neurosurgery is important.

In the search for noninvasive methods that yield this information, magnetoencephalography (MEG) (1,5–13) and functional magnetic resonance (MR) imaging (2,8,9,12–30) have been particular focuses of interest. MEG and functional MR imaging have been compared in a clinical setting for their effectiveness in central sulcus localization in only a few studies (8,9,12,13). Although the performances of these two methods have been consistent with each other and with those of invasive cortical mapping in most cases, discrepancies have been reported (9). Thus, the purpose of this study was to prospectively evaluate MEG and functional MR imaging, as compared with intraoperative cortical mapping, for identification of the central sulcus.

Materials and Methods

One author (M.S.) operates a software company that has sold visualization software to Elekta Neuromag (Helsinki, Finland), the manufacturer of the magnetometer used in this study. The rest of the authors, who have no direct or indirect financial interest in Elekta Neuromag, had control over the inclusion of any manuscript data and information that might have represented a conflict of interest for M.S.

Advances in Knowledge

- In our study, magnetoencephalography was found to be superior to functional MR imaging for identification of the central sulcus.
- The results of motor functional MR imaging can be confounded by activations in multiple nonprimary areas.

Patients

Fifteen patients (six men, nine women; age range, 25–58 years) with a lesion near the primary sensorimotor cortex (13 gliomas, one cavernous hemangioma, and one meningioma) were examined after institutional review board approval and written informed consent from each patient were obtained. Subjects who were consecutive patients of one neurosurgeon (J.E.J.), had a lesion near the primary sensorimotor cortex, and were scheduled for surgery by means of awake craniotomy and monitoring with intraoperative cortical mapping were recruited from February 1998 through November 1999. The area of the primary sensorimotor cortex that controls hand function was mapped preoperatively with functional MR imaging and MEG and was mapped intraoperatively by means of cortical stimulation and/or recording of the cortical somatosensory evoked potentials.

MR Image Acquisition and Data Analysis

MR images were acquired with a 1.5-T Vision system (Siemens Medical Systems, Erlangen, Germany) by using a standard head coil. One transverse, one coronal, and three sagittal localizer images were acquired for section positioning. In each patient, a set of 1-mm-thick contiguous sagittal T1-weighted whole-head images (field of view, 256 mm; matrix, 256 × 256) was obtained by using a three-dimensional (3D) magnetization-prepared rapid gradient-echo sequence (repetition time msec/echo time msec/inversion time msec, 9.7/4/20; flip angle, 10°) before and after the administration of a gadolinium-based contrast agent: gadopentetate dimeglumine (Magnevist; Schering, Berlin, Germany) or gadoterate meglumine (Dotarem; Guerbet, Roissy, France). In each patient, 16 3-mm-thick contiguous transverse functional MR image sections were obtained by using a gradient-echo echo-planar sequence (repetition time msec/echo time msec, 3500/70; flip angle, 90°; field of view, 256 mm; matrix, 128 × 128) to cover the area of the primary sensorimotor cortex that controls hand function. The functional MR imaging paradigm included periods of self-paced palmar hand flexions contralateral to the lesion, which were alternated with rest. A time series of 91–128 volumes of gradient-echo echo-planar images was acquired.

For functional MR imaging analysis and coregistration of the functional images with the structural images, we used FSL 3.1 (Oxford Centre for Functional Magnetic Resonance Imaging of the Brain, John Radcliffe Hospital, Headington, Oxford, England) and in-house software. The images were first corrected for motion (31). To reach a steady state of longitudinal magnetization, we discarded the first two image volumes. Mean-based intensity normalization of all volumes, performed by using the same factor, and nonlinear high-pass temporal filtering (ie, Gaussian-weighted least-squares straight-line fitting, σ = 52.5 seconds) were performed. Thereafter, statistical images were generated. Functional MR imaging results were visualized by showing them as pseudocolor overlays on three orthogonal views and on 3D reconstruc-

Published online before print
10.1148/radiol.2411050796

Radiology 2006; 241:213–222

Abbreviations:
ECD = equivalent current dipole
MEG = magnetoencephalography
N20m = first cortical somatosensory evoked response component
3D = three-dimensional

Author contributions:
Guarantors of integrity of entire study, A.K., H.J.A., J.H.; study concepts/study design or data acquisition or data analysis/interpretation, all authors; manuscript drafting or manuscript revision for important intellectual content, all authors; manuscript final version approval, all authors; literature research, A.K., E.K., H.J.A., S.A., J.H., R.J.I., J.E.J., J.P.M.; clinical studies, A.K., E.K., S.A., A.B., J.E.J., T.K., J.P.M.; statistical analysis, A.K., E.K., H.J.A., S.A., J.P.M., E.S., M.S.; and manuscript editing, all authors

See Materials and Methods for pertinent disclosures.

tions of segmented (32) images by using MRIcro software written by Chris Rorden *(http://www.sph.sc.edu/comd/rorden/mricro.html)* (33). The software is distributed as freeware by the author. By using the atlas of Duvernoy (34), one of the authors (A.K., with 10 years experience in brain MR imaging) labeled the activation according to the nearest sulcus and gyrus. The location of the central sulcus determined intraoperatively served as the reference. The same author (A.K.) manually outlined the tumor. Thereafter, the shortest Euclidian distance between the area of the peak statistical value in the central sulcus and the tumor margin was calculated.

MEG Recordings and Data Analysis

With use of a 122- or 306-channel helmet-shaped magnetometer (Neuromag 122 and Neuromag VectorView, respectively; Elekta Neuromag) in a magnetically shielded room (Euroshield, Eura, Finland), MEG responses to median nerve stimulation contralateral to the lesion were recorded. Constant-current 0.2-msec pulses were delivered at 2 Hz to the wrist at an intensity slightly above the motor threshold. The signals were band-pass filtered (0.03–320.00 Hz) before sampling at 987 Hz. The sweep duration of 550 msec included a 50-msec prestimulus baseline. Epochs containing MEG amplitudes higher than 3000 fT/m or electric ocular or muscle artifacts exceeding 150 μV were rejected from the averaging. About 200 responses were recorded for each averaged trace.

The preauricular points and the nasion, as well as four head-position indicator coils attached to the patient's head, were located with a 3D digitizer (Polhemus, Colchester, Vt). The anatomic landmarks were marked on the skin with a pen and photographed for later reference. We determined the

Table 1

Characteristics, Lesion Features, and Pre- and Postoperative Symptoms of Patients

Patient No./Sex/Age (y)*	Lesion Type†	Lesion Location‡	Preoperative Status	Postoperative Status	
				<1 Week	>1 Month
1/F/26	WHO type 2 astrocytoma	L frontoparietal	Mild dysphasia	Moderate dysphasia	Mild dysphasia
2/F/55	Cavernous hemangioma	R parietal	No deficits	No deficits	No deficits
3/M/48	WHO type 2 astrocytoma	L parietal	Mild dysphasia	Moderate dysphasia	Mild dysphasia
4/F/49	WHO type 2 oligodendroglioma	Bilateral frontal	No deficits	Severe dysphasia, moderate right upper limb hemiparesis	Mild dysphasia, mild right hemiparesis
5/F/51	WHO type 4 glioblastoma	R frontal	No deficits	Mild left hemiparesis	Left proprioceptive apraxia
6/M/25	WHO type 2 astrocytoma	R parietal	No deficits	No deficits	No deficits
7/M/43	WHO type 3 oligoastrocytoma	L temporal	Mild right hemiparesis, memory impairment, dysphasia	Moderate right hemiparesis, memory impairment, dysphasia	Moderate right hemiparesis, memory impairment, dysphasia
8/F/52	WHO type 2 glioma	L parietal	Mild right upper limb apraxia	Moderate right upper limb apraxia, mild dysphasia	Mild right upper limb apraxia, dysphasia
9/M/40	WHO type 2 glioma	R frontal	Mild left proprioceptive hemiapraxia	Mild left limb apraxia	Mild left apraxia
10/F/47	Meningioma	R parasagittal parietal	No deficits	Mild left lower limb paresis	No deficits
11/F/58	WHO type 4 glioblastoma	L temporal	Mild dysphasia	Moderate dysphasia	Mild dysphasia
12/F/49	WHO type 2 astrocytoma	R frontoparietal	No deficits	Mild left upper limb apraxia	Mild left upper limb apraxia
13/F/41	WHO type 2 glioma	R frontal	Mild right hand parestesia, right hemiparesis	Mild right hand parestesia and hemiparesis	
14/M/50	WHO type 2 astrocytoma	R frontal	No deficits	No deficits	No deficits
15/M/35	WHO type 2 glioma	R frontal	No deficits	Mild left upper limb apraxia	

* Patients 1, 3, 4, 7, and 13 had undergone surgery previously.

† WHO = World Health Organization.

‡ L = left, R = right.

head position within the magnetometer helmet by allowing a current to pass through the indicator coils and recording the induced magnetic signals.

The head was modeled by a spherical conductor that matched the local curvature of the inner surface of the skull in the region of interest. A least-squares search revealed the equivalent current dipole (ECD) that best accounted for the measured magnetic fields at the given time point. The search was performed over a time window that corresponded to the first cortical somatosensory evoked response component (N20m). A local subset of 27–44 channels was used for fitting.

The data for patient 4 were digitally high-pass filtered at 10 Hz to remove slow artifacts that arose from magnetic items inside the head (ie, steel splinters from surgical drills). For patients 1 and 15, respectively, 145- and 140-Hz low-pass filters were used to remove 150-Hz noise. For patient 1, a 50-Hz notch filter was used to remove 50-Hz noise.

One author (A.K.) coregistered the MEG coordinate space with the T1-weighted 3D magnetization-prepared rapid gradient-echo MR images by identifying the digitized anatomic landmarks on these images. A 3D volume-rendered image was created from the contrast agent–enhanced image set that depicted the cortical surface, cortical veins, and ECD.

Figure 1

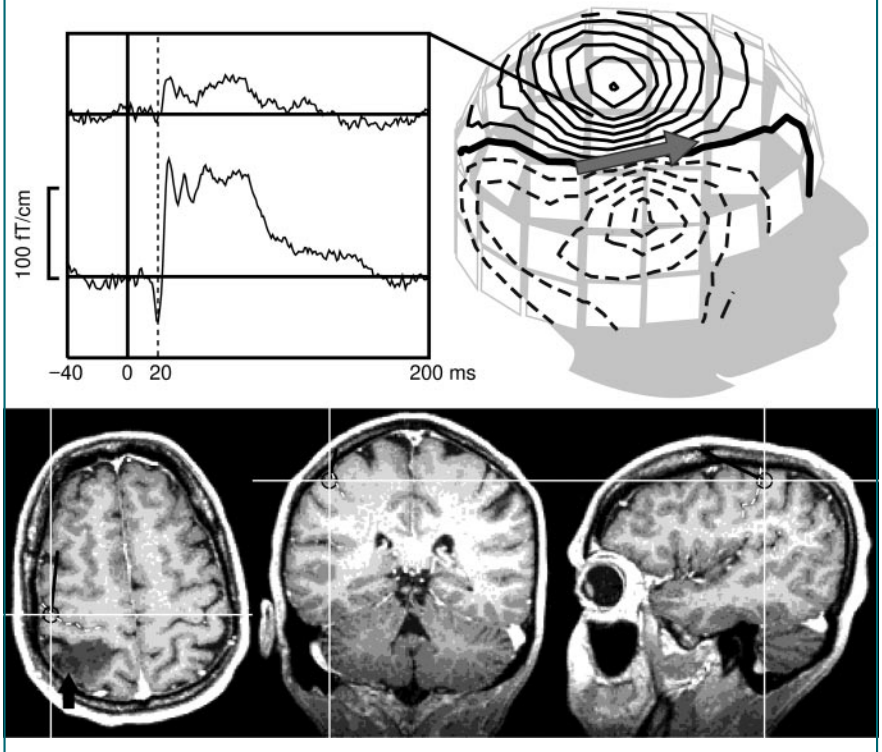

Figure 1: Somatosensory evoked magnetic fields after left median nerve stimulation in patient 12, who had parietal glioma (arrow, bottom left image). Top left: Individual response waveforms from two channels over the right sensorimotor cortex are shown; dashed vertical line marks the 20-msec component known to be generated in the postcentral wall of the central sulcus (Brodmann area 3b). Stimuli were applied at 0 msec. Top right: Corresponding isofield contour map (contour step, 20 fT) shows dipolar distribution of the magnetic field. Solid lines over helmet-shaped sensor array (white squares) represent magnetic field exiting the head; dashed lines represent magnetic field entering the head. Arrow depicts ECD fitted to the field distribution. Bottom: Dipole location is shown on transverse (left), coronal (middle), and sagittal (right) MR images in same patient. Position of dipole is illustrated by crosshairs and circled; line crossing shows dipole orientation. Dashed lines mark the central sulcus, as identified at intraoperative mapping.

Intraoperative Monitoring

Intraoperative electrophysiologic monitoring was performed during awake craniotomy (E.K., T.K., and J.E.J., with 1, 3, and 3 years experience, respectively). Somatosensory evoked potential recording and cortical stimulation were performed in seven patients. Only cortical stimulation was performed in seven patients. In one patient, only somatosensory evoked potential recording was performed.

Cortical stimulation and evoked potential recording were performed by using an eight-channel Viking IV recorder (Nicolet Biomedical, Madison, Wis). For somatosensory evoked potential recording, the median nerve was stimulated at the wrist with 0.2-msec constant-current pulses at 4 Hz, with the stimulus intensity exceeding the motor threshold. Responses were recorded from the first two rows of a 4 × 5-electrode grid (PMT, Chanhassen, Minn) with 3-mm spacing and 6.5-mm-diameter silver–silver chloride electrodes. A reference needle electrode was inserted into the temporal muscle on the surgically treated side. At cortical stimulation, 50-Hz electric pulses (duration, 0.2 msec; intensity, 6–13 mA) were used.

Delineation of the Central Sulcus

The ECD locations determined by using MEG were superimposed on the MR image sections. If the ECD was located in a gyrus, the sulcus nearest to this location in the dipolar direction was labeled as the central sulcus. If the ECD was located in a sulcus, this sulcus was considered to be the central sulcus.

At functional MR imaging, two criteria were used separately to identify the central sulcus: the sulcus with the largest number of activated voxels and the sulcus nearest to the area of the maximal z-statistic value. At electrocorticography, the central sulcus was identified by using the phase reversal of the 20–25-msec response between the electrodes located frontally and parietally.

During the cortical stimulation, the

motor responses were monitored and the patients were asked to report their sensations. The central sulcus was identified as the sulcus posterior to the gyrus from which the stimulation elicited motor responses. The exposed cortex was photographed before and after application of the tags or the corticographic electrode grid.

The central sulcus was delineated at MEG and functional MR imaging by A.K. and was delineated intraoperatively by A.K., E.K., and J.E.J. in consensus. The Euclidian distance from the N20m ECD to both the nearest functional MR imaging activation voxel and the maximal *z*-score voxel was considered the measure of the MEG and functional MR imaging overlap.

Statistical Analyses

Statistical analysis of the functional MR imaging data was performed by using a general linear model with local autocorrelation correction (35). *z*-Statistic (ie, Gaussianized *t*) images were segmented into activated and nonactivated regions by means of contextual clustering (36,37). Parameters (initial thresholding $z > 1.6$, neighborhood weighting $\beta = 0.427$) (33) that would yield an approximate global false-positive rate of 0.01 in a search volume of the brain on the echo-planar MR images were chosen. For analysis of the MEG data, the percentage of variance explained by ECDs—that is, the goodness of fit—and the 95% confidence volume for ECD location were calculated (38). The distance from the area of maximal functional MR imaging activation near the central sulcus to the tumor margin was measured in each patient. The difference in this distance between the patients with functional MR imaging results concordant with intraoperative mapping and those with discordant results was evaluated by using an unpaired one-sided *t* test.

Results

Delineation of the Central Sulcus

In all 15 patients (Table 1), MEG depicted the central sulcus correctly (Figs 1–4). When the data for patient 1, which contained more noise, were removed as an outlier, the goodness of fit of the N20m ECDs ranged from 88.8% to 98.2% (mean, 94.4%). The 95% confidence volumes for the ECDs ranged from 42 to 1001 mm^3 (mean, 478 mm^3), with the exception of the ECD 95% confidence volume for patient 1, which was 25 098 mm^3; the goodness of fit was 64.1%.

In 11 (73%) patients, the area of primary activation at functional MR imaging was concordant with that at MEG and intraoperative mapping (Fig 2), whereas in four (27%) patients, the area of primary activation at functional MR imaging occurred in the region of the postcentral sulcus (Table 2, Figs 3, 4). The MEG dipole was always within 1–6 mm from the nearest functional MR imaging activation voxel and within 6–36 mm from the maximal *z*-score voxel (Table 2). There was no consistent difference in the proximity of the lesion to the central sulcus between the group of four patients in whom the dominant functional MR imaging activation occurred in the postcentral sulcus and the remaining patients (Table 2). The lesion–central sulcus distance ranged from 3 to 34 mm (mean, 13 mm) in the cases in which the dominant activation

Figure 2

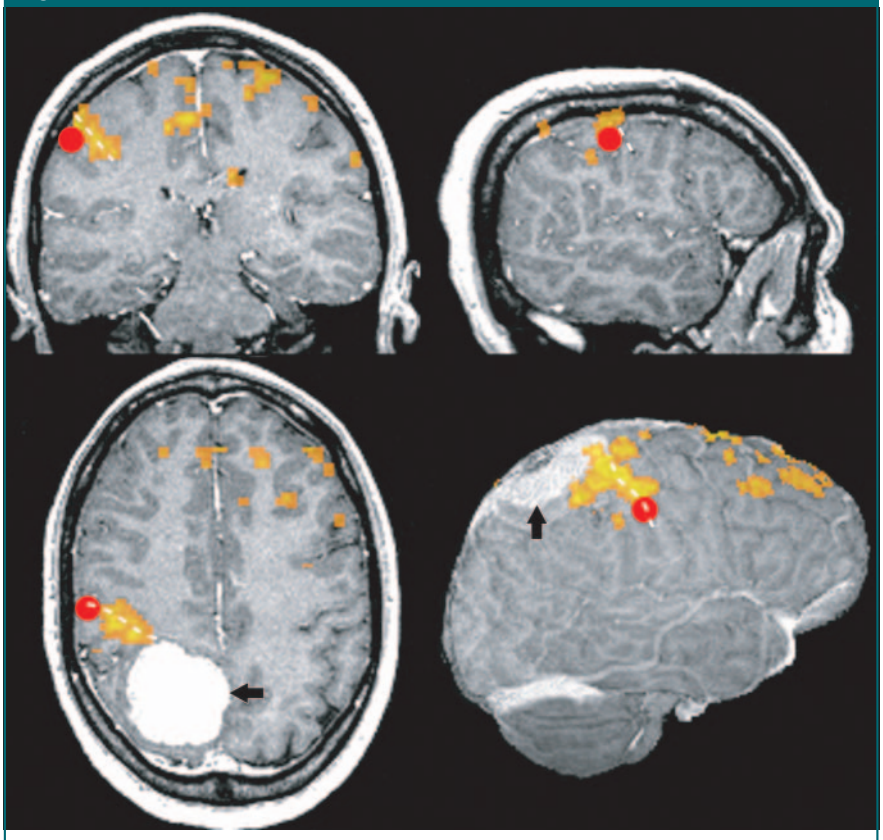

Figure 2: Functional MR imaging activations and MEG dipole location in patient 10, who had parietal meningioma (arrows). Activations (orange) are shown with pseudocolor overlays on 3D surface reconstruction of contrast-enhanced 3D magnetization-prepared rapid gradient-echo image volume (bottom right) and on sagittal (top right), coronal (top left), and transverse (bottom left) image sections through primary sensorimotor cortex in right hemisphere. N20m dipole location is seen in postcentral gyrus (red dots). Both functional MR imaging and MEG correctly depicted the central sulcus in this patient. Activations are seen, in addition to in the primary sensorimotor cortex, in the frontal and posterior parietal cortices and in areas of the interhemispheric fissure walls. The meningioma has intense and homogeneous gadolinium enhancement. Central sulcus location, as verified at intraoperative mapping, is marked by dashed line.

occurred in the postcentral sulcus and from 0 to 49 mm (mean, 21 mm) in the cases in which the dominant activation occurred in the central sulcus, with no significant difference between the group means ($P = .38$). The results were the same, regardless of the decision criteria used to interpret the functional MR imaging finding. The two intraoperative mapping methods yielded consistent results in all seven patients who were examined with both methods.

Activated Areas at Functional MR Imaging

In the hemisphere contralateral to the movement, the precentral gyrus within the central sulcus wall was activated in all patients. In all patients except patient 14, activation was seen also in the postcentral gyrus within the central sulcus. In 10 patients, activation was seen in the precentral gyrus, as well as in the superior, medial, and inferior frontal gyri within the precentral sulcus. In 13 patients, activation was observed in the postcentral, superior parietal, and supramarginal gyri within the postcentral sulcus.

More rostrally, activation was observed in the superior (seven patients), middle (three patients), and inferior frontal (two patients) sulci. In addition, parietal activations were observed in the superior parietal, angular, and supramarginal gyri within the intraparietal sulcus in 12 patients. Activations were observed in the supramarginal gyri within the lateral sulcus in five patients.

Ipsilaterally, activations were seen in the precentral wall (11 patients) and on the postcentral side (six patients) of the central sulcus. Precentral gyrus activations in the precentral sulcus and activations in the postcentral, superior parietal, and supramarginal gyri within the postcentral sulcus were seen in nine patients. In addition, activations were seen in the ipsilateral superior (10 patients), middle (four patients), and inferior (four patients) frontal sulci, as well as in the intraparietal (12 patients) and lateral (six patients) sulci.

Within the interhemispheric fissure, activations were seen in either or both hemispheres in the medial aspect of the superior frontal gyrus (13 patients) and the fissural part of the superior frontal gyrus (11 patients) in the cingulate sulcus. Activation was seen also in the paracentral lobule ($n = 6$), cingulate gyrus ($n = 9$), and fissural part of the postcentral gyrus (three patients) in the cingulate sulcus.

Figure 3

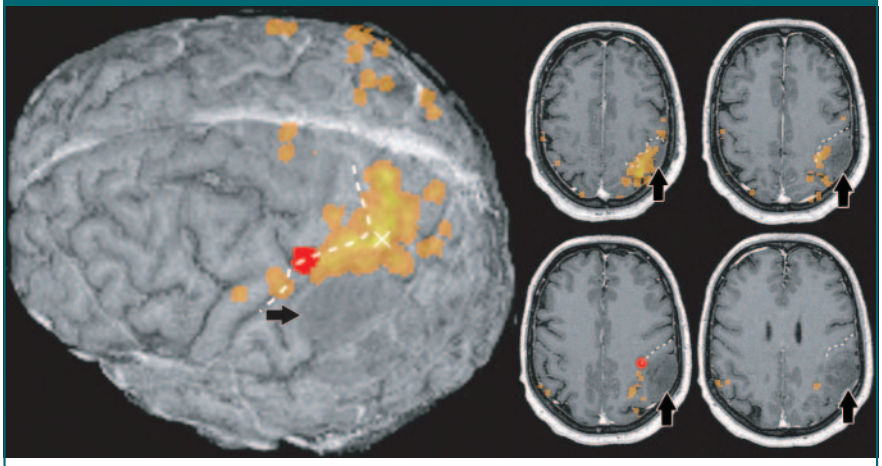

Figure 3: Activations and MEG dipole location (red areas) on functional MR images (pseudocolor maps) in patient 8, who had parietal glioma (arrows). Three-dimensional surface reconstruction of contrast-enhanced 3D magnetization-prepared rapid gradient-echo image volume (left) and four transverse image sections (right) through primary sensorimotor cortex are shown. Largest activation area was in postcentral sulcus and extended contiguously to central sulcus (dashed line). Area of peak statistical value (×, left image) also was in postcentral sulcus region. Other activations in precentral superior parietal gyrus and supplementary motor area are visible in left hemisphere. Central sulcus location, as verified at intraoperative mapping, is marked by dashed line.

Discussion

In this study, we used the most widely applied paradigms for MEG and functional MR imaging for primary sensorimotor cortex localization, which is a motor task at functional MR imaging and an electric stimulation of a peripheral nerve at MEG. In our study, MEG enabled more reliable localization of the central sulcus compared with functional MR imaging. According to our study results, in some cases motor activation at functional MR imaging may occur predominantly in nonprimary areas—the postcentral sulcus in particular. In this study, the problems associated with activation in nonprimary areas did not occur with MEG, with which the earliest component of the evoked response arising from the primary somatosensory cortex can be separated from later parts of the response, which arise partly in nonprimary areas (39–41).

The superiority of MEG in the temporal domain is due to the fact that this examination enables one to directly measure neuronal electrical activity in a millisecond time scale, whereas functional MR imaging is based on the measurement of hemodynamic responses that reflect neuronal activation, which are much longer than the underlying neuronal activity, lasting up to 15 seconds after a stimulus (42).

In suitable conditions—for example, when a single spatially confined source area is activated—5-mm spatial resolution can be achieved with MEG in practical applications (43,44). Typical spatial resolutions at functional MR imaging studies of presurgical mapping have ranged from 3 to 4 mm in a plane with a section thickness of 5–6 mm (45). Hence, although the spatial resolution achieved with both techniques can be high, functional MR imaging can be considered superior in the spatial domain. This is especially evident in the capability of functional MR imaging to reveal spatial details of the activation—even at

the cortical column level (46)—and activations extending over large areas of the cortex. At MEG, the ECD represents an estimate of the center of gravity of the underlying activation, which may have considerable dimensions (38). Even the use of more sophisticated source models, such as minimum-norm estimates, has not enabled reliable reproduction of the spatial details of the underlying activation at MEG examinations.

The spatial specificity of functional MR imaging, however, depends on the type of technique used. Gradient-echo MR imaging of the oxygenation state is known to be sensitive to signals arising from the veins that drain the activated cortex. Approaches based on imaging of the cerebral blood flow or volume offer better spatial specificity (47)—but at the price of a lower signal-to-noise ratio, which has limited practical use with these techniques. This better spatial specificity, however, does not solve the problem of the activation in adjacent nonprimary functional areas. The analysis methods used also influence the sensitivity and spatial specificity of functional MR imaging.

The spatial accuracies of MEG and functional MR imaging are dependent on the procedures used to coregister the functional data with the structural image data. Spatial distortions due to susceptibility effects are common with functional MR imaging. On the other hand, the landmark-based registration used with MEG can involve human-induced errors.

Despite the limited spatial resolution of MEG compared with the spatial resolution of functional MR imaging, our results confirm the amply documented suitability of somatosensory evoked magnetic fields for localization of the central sulcus (1,5,6,8–13,48,49). In fact, in all 175 patients examined in previous studies (1,5,6,8–13,48,49) and in all 15 patients examined in our study, localization of the central sulcus with MEG was correct. The localization information gleaned from somatosensory evoked magnetic field recording can even be corroborated with the information obtained at primary motor cortex localization by measuring the coherence between cortical oscillations and electromyography (10).

Figure 4

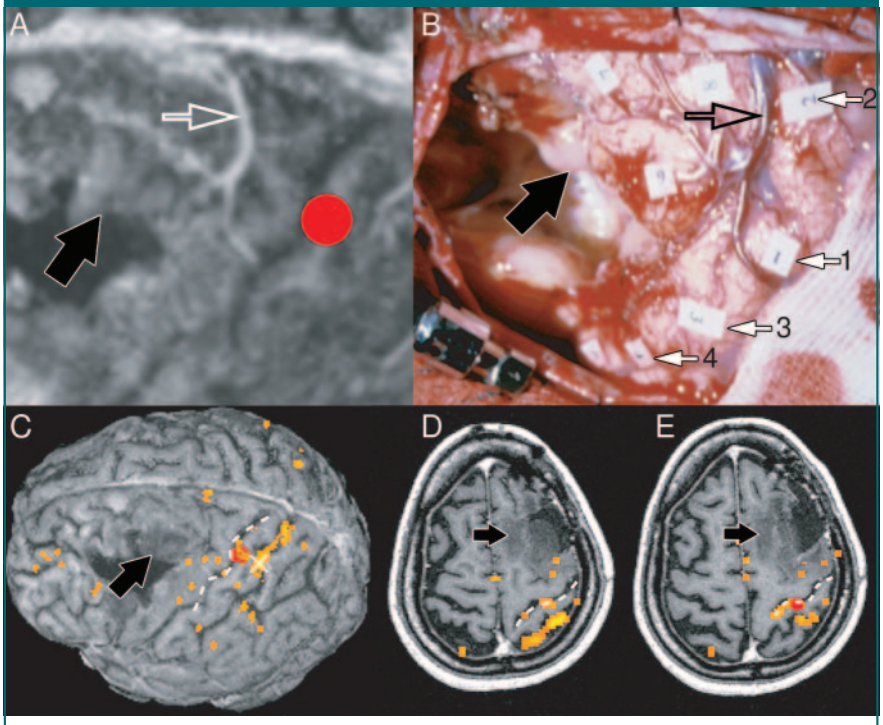

Figure 4: *A,* Part of 3D surface reconstruction of contrast-enhanced magnetization-prepared rapid gradient-echo MR image volume in patient 1 shows MEG dipole location (red dot) in postcentral gyrus and a cortical vein (open arrow) that can be identified also on the intraoperative view *(B)* of the brain surface in the same patient. This patient underwent repeat surgery of the residual tumor (Word Health Organization type 2 astrocytoma, solid black arrow in *A–E*) within the surgical cavity in left frontal lobe. The cortex was stimulated at labeled sites *1–4*. Stimulation at sites *1* and *2* caused contraction of hand muscles; stimulation at sites *3* and *4* caused a motor response in mouth area. *C,* Brain surface at functional MR imaging activation during motor task and N20m dipole location at MEG (red areas in *C* and *E*). × marks location of peak value (area of highest *z* score) depicted on functional MR imaging statistical activation map. In left hemisphere, activation is also seen in supramarginal gyrus and in medial and inferior frontal gyri. *D, E,* Transverse cranial *(D)* and caudal *(E)* MR image sections through primary sensorimotor cortex show bulk of functional MR activation in postcentral sulcus region. In *C–E*, central sulcus location, as verified at intraoperative mapping, is marked by dashed line.

With functional MR imaging, the activation of multiple nonprimary areas during a motor task is an expected finding, according to previous imaging results for healthy subjects (50–52). However, the effect of these activations on the interpretation of functional MR imaging motor activation patterns has received little attention in previous studies involving patients. Data in the bulk of the current literature suggest that the primary sensorimotor cortex can be located reliably with functional MR imaging by using a motor task (2,8,12–18,20,21,23,25–30,53), and nonprimary activations are not appreciated as a confounding factor in these reports. In contrast, the results of this study, in agreement with the findings of some previous studies involving limited numbers of patients (9,17,19), indicate that widespread functional MR imaging activation may render identification of the central sulcus difficult.

Even simple limb movements require the concerted action of multiple motor and somatosensory cortical areas. In the motor cortical network, primary motor, premotor, and supplementary motor areas are activated to a variable degree in most subjects. Somatosensory afferent signals provide in-

dispensable feedback information that is necessary for the execution of all kinds of movements. Also, simple flexion-extension movements, such as those used in our study and in most previous studies, necessarily activate different types of afferent nerve fibers, including proprioceptive afferent fibers. In the cortex, the proprioceptive afferent fibers are largely relayed to Brodmann areas 2 and 5 (54), which are located in the postcentral sulcus region. It is therefore not surprising that functional MR imaging activations extended to—and in some patients occurred predominantly in—the postcentral sulcus area.

The observed interindividual variations in functional MR imaging activation patterns could have also reflected the variable strategies used to perform the motor tasks among the patients with brain lesions. It has been suggested that brain abnormalities may also contribute to variations in activation by means of either mechanical effects (27) or modulation of the neurovascular coupling through neurotransmitters and tumor invasion of the functional cortex. There have also been observations that contradict these views (54,55). In this study, there was no difference in the proximity of the lesion to the central sulcus between the patients with false and those with correct localization results.

The interpreter of the functional MR imaging results can use previous experience and knowledge of anatomic landmarks in combination with the functional map of the sensorimotor network. This kind of a priori information, however, is not always available—for example, in cases in which the anatomy has been distorted by a lesion or lesions. It is in these cases that information about the functional anatomy is most valuable.

Our study had limitations. It included a small patient group. The types and locations of the lesions varied considerably. These factors hinder the evaluation of the contribution of possible tumor-induced neurovascular uncoupling effects to the false localization results. Because stereotactic neuronavigation was not available at the time of the study, our investigation was limited to the identification of the central sulcus; no quantitative measurements of the overlap of intraoperative mapping with noninvasive methods were made.

The results of our study emphasize that the limited temporal resolution must be appreciated when interpreting functional MR imaging results. Because functional MR imaging is more accessible than is MEG, it will likely remain the primary method used for noninvasive functional mapping. Ultimately, it may be beneficial to use both methods, if feasible (9,56), to achieve the most complete and reliable characterization of the functional anatomy.

Acknowledgments: We thank Riitta Hari, MD, PhD, and Nina Forss, MD, PhD, for their support and helpful suggestions during the study.

Table 2

Agreement of MEG and Functional MR Imaging Findings with Intraoperative Mapping Findings or Anatomic Landmarks

Patient No.	Intraoperative Localization Method*	Sulcus Identified as CS at Functional MR†		Distance from Functional MR Central Sulcus Activation to Tumor (mm)	N20m-ECD Distance (mm)‡	
		Largest Activation Area	Highest *z* Score Area		To Closest Functional MR Voxel	To Highest *z* Score Area
1	COS, ECoG	PCS	PCS	10	0	25
2	COS, ECoG	CS	CS	39	1	36
3	COS	CS	CS	49	4	20
4	COS	CS	CS	16	0	6
5	COS, ECoG	CS	CS	48	5	27
6	COS, ECoG	CS	CS	4	1	28
7	COS	PCS	PCS	3	0	23
8	ECoG	PCS	PCS	4	5	27
9	COS, ECoG	PCS	PCS	34	5	27
10	COS, ECoG	CS	CS	7	2	25
11	COS	CS	CS	30	0	21
12	COS, ECoG	CS	CS	15	1	29
13	COS	CS	CS	3	0	14
14	COS	CS	CS	7	6	13
15	COS	CS	CS	0	3	8

Note.—The spatial extent (ie, largest activation) and the global maximum of the statistical parameter map (ie, highest *z* score) were used as independent criteria in the identification of the central sulcus and were consistent in all cases. The proximity of the tumor margin to the central sulcus did not exhibit any relation to the mapping results.

* COS = cortical stimulation, ECoG = electrocorticography.

† The central sulcus (CS) was correctly identified at MEG in all 15 patients. PCS = postcentral sulcus.

‡ Distance from MEG dipole location to closest functional MR imaging activation.

References

1. Sobel DF, Gallen CC, Schwartz BJ, et al. Locating the central sulcus: comparison of MR anatomic and magnetoencephalographic functional methods. AJNR Am J Neuroradiol 1993;14:915–925.
2. Towle VL, Khorasani L, Uftring S, et al. Noninvasive identification of human central sulcus: a comparison of gyral morphology, functional MRI, dipole localization, and direct cortical mapping. Neuroimage 2003;19:684–697.
3. Wunderlich G, Knorr U, Herzog H, Kiwit JC, Freund HJ, Seitz RJ. Precentral glioma location determines the displacement of cortical hand representation. Neurosurgery 1998;42:18–26.
4. Vates GE, Lawton MT, Wilson CB, et al. Magnetic source imaging demonstrates altered cortical distribution of function in patients with arteriovenous malformations. Neurosurgery 2002;51:614–623.
5. Sutherling WW, Crandall PH, Darcey TM, Becker DP, Levesque MF, Barth DS. The magnetic and electric fields agree with intracranial localizations of somatosensory cortex. Neurology 1988;38:1705–1714.
6. Rezai AR, Hund M, Kronberg E, et al. The interactive use of magnetoencephalography in stereotactic image-guided neurosurgery. Neurosurgery 1996;39:92–102.
7. Hund M, Rezai AR, Kronberg E, et al. Magnetoencephalographic mapping: basic of a new functional risk profile in the selection of patients with cortical brain lesions. Neurosurgery 1997;40:936–942.
8. Nimsky C, Ganslandt O, Kober H, et al. Integration of functional magnetic resonance imaging supported by magnetoencephalography in functional neuronavigation. Neurosurgery 1999;44:1249–1255.
9. Inoue T, Shimizu H, Nakasato N, Kumabe T, Yoshimoto T. Accuracy and limitation of functional magnetic resonance imaging for identification of the central sulcus: comparison with magnetoencephalography in patients with brain tumors. Neuroimage 1999;10:738–748.
10. Mäkelä JP, Kirveskari E, Seppä M, et al. Three-dimensional integration of brain anatomy and function to facilitate intraoperative navigation around the sensorimotor strip. Hum Brain Mapp 2001;12:180–192.
11. Ganslandt O, Fahlbusch R, Nimsky C, et al. Functional neuronavigation with magnetoencephalography: outcome in 50 patients with lesions around the motor cortex. J Neurosurg 1999;91:73–79.
12. Kober H, Nimsky C, Möller M, Hastreiter P, Fahlbusch R, Ganslandt O. Correlation of sensorimotor activation with functional magnetic resonance imaging and magnetoencephalography in presurgical functional imaging: a spatial analysis. Neuroimage 2001;14:1214–1228.
13. Kamada K, Houkin K, Takeuchi F, et al. Visualization of the eloquent motor system by integration of MEG, functional, and anisotropic diffusion-weighted MRI in functional neuronavigation. Surg Neurol 2003;59:352–361.
14. Jack CR Jr, Thompson R, Butts R, et al. Sensory motor cortex: correlation of presurgical mapping with functional MR imaging and invasive cortical mapping. Radiology 1994;190:85–92.
15. Puce A, Constable RT, Luby ML, et al. Functional magnetic resonance imaging of sensory and motor cortex: comparison with electrophysiological localization. J Neurosurg 1995;83:262–270.
16. Yousry TA, Schmid UD, Jassoy AG, et al. Topography of the cortical motor hand area: prospective study with functional MR imaging and direct motor mapping at surgery. Radiology 1995;195:23–29.
17. Yousry TA, Schmid UD, Schmidt D, Hagen T, Jassoy A, Reiser MF. The central sulcal vein: a landmark for identification of the central sulcus using functional magnetic resonance imaging. J Neurosurg 1996;85:608–617.
18. Mueller WM, Yetkin FZ, Hammeke TA, et al. Functional magnetic resonance imaging mapping of the motor cortex in patients with cerebral tumors. Neurosurgery 1996;39:515–520.
19. Pujol J, Conesa G, Deus J, et al. Presurgical identification of the primary sensorimotor cortex by functional magnetic resonance imaging. J Neurosurg 1996;84:7–13.
20. Pujol J, Conesa G, Deus J, López-Obarrio L, Isamat F, Capdevila A. Clinical application of functional magnetic resonance imaging in presurgical identification of the central sulcus. J Neurosurg 1998;88:863–869.
21. Krings T, Buchbinder BR, Butler WE, et al. Functional magnetic resonance imaging and transcranial magnetic stimulation: complementary approaches in the evaluation of cortical motor function. Neurology 1997;48:1406–1416.
22. Krings T, Reinges MH, Erberich S, et al. Functional MRI for presurgical planning: problems, artefacts, and solution strategies. J Neurol Neurosurg Psychiatry 2001;70:749–760.
23. Schulder M, Maldjian JA, Liu WC, et al. Functional image-guided surgery of intracranial tumors located in or near the sensorimotor cortex. J Neurosurg 1998;89:412–418.
24. Fandino J, Kollias SS, Wieser HG, Valavanis A, Yonekawa Y. Intraoperative validation of functional magnetic resonance imaging and cortical reorganization patterns in patients with brain tumors involving the primary motor cortex. J Neurosurg 1999;91:238–250.
25. Roux FE, Boulanouar K, Ranjeva JP, et al. Usefulness of motor functional MRI correlated to cortical mapping in Rolandic low-grade astrocytomas. Acta Neurochir (Wien) 1999;141:71–79.
26. Hirsch J, Ruge MI, Kim KH, et al. An integrated functional magnetic resonance imaging procedure for preoperative mapping of cortical areas associated with tactile, motor, language, and visual functions. Neurosurgery 2000;47:711–721.
27. Holodny AI, Schulder M, Liu WC, Wolko J, Maldjian JA, Kalnin AJ. The effect of brain tumors on BOLD functional MR imaging activation in the adjacent motor cortex: implications for image-guided neurosurgery. AJNR Am J Neuroradiol 2000;21:1415–1422.
28. Krings T, Schreckenberger M, Rohde V, et al. Metabolic and electrophysiological validation of functional MRI. J Neurol Neurosurg Psychiatry 2001;71:762–771.
29. Lehéricy S, Duffau H, Cornu P, et al. Correspondence between functional magnetic resonance imaging somatotopy and individual brain anatomy of the central region: comparison with intraoperative stimulation in patients with brain tumors. J Neurosurg 2000;92:589–598.
30. Krings T, Schreckenberger M, Rohde V, et al. Functional MRI and 18F FDG-positron emission tomography for presurgical planning: comparison with electrical cortical stimulation. Acta Neurochir (Wien) 2002;144:889–899.
31. Jenkinson M, Bannister P, Brady M, Smith S. Improved optimization for the robust and accurate linear registration and motion correction of brain images. Neuroimage 2002;17:825–841.
32. Smith SM. Fast robust automated brain extraction. Hum Brain Mapp 2002;17:143–155.
33. Rorden C, Brett M. Stereotaxic display of brain lesions. Behav Neurol 2000;12:191–200.
34. Duvernoy HM. The human brain: surface, three-dimensional sectional anatomy with MRI, and blood supply. 2nd ed. Vienna, Austria: Springer-Verlag, 1999.

35. Woolrich MW, Ripley BD, Brady M, Smith SM. Temporal autocorrelation in univariate linear modeling of FMRI data. Neuroimage 2001;14:1370–1386.

36. Salli E, Aronen HJ, Savolainen S, Korvenoja A, Visa A. Contextual clustering for analysis of functional MRI data. IEEE Trans Med Imaging 2001;20:403–414.

37. Salli E, Korvenoja A, Visa A, Katila T, Aronen HJ. Reproducibility of fMRI: effect of the use of contextual information. Neuroimage 2001;13:459–471.

38. Hämäläinen M, Hari R, Ilmoniemi RJ, Knuutila J, Lounasmaa OV. Magnetoencephalography: theory, instrumentation, and applications to noninvasive studies of the working human brain. Rev Mod Phys 1993;65:413–497.

39. Hari R, Karhu J, Hämäläinen M, et al. Somatosensory evoked cerebral magnetic fields from SI and SII in man. Eur J Neurosci 1984; 57:254–263.

40. Forss N, Hari R, Salmelin R, et al. Activation of the human posterior parietal cortex by median nerve stimulation. Exp Brain Res 1994;99:309–315.

41. Forss N, Merlet I, Vanni S, Hämäläinen M, Mauguière F, Hari R. Activation of human mesial cortex during somatosensory target detection task. Brain Res 1996;734:229–235.

42. Glover GH. Deconvolution of impulse response in event-related BOLD fMRI. Neuroimage 1999;9:416–429.

43. Virtanen J, Ahveninen J, Ilmoniemi RJ, Näätänen R, Pekkonen E. Replicability of MEG and EEG measures of the auditory N1/N1m-response. Electroencephalogr Clin Neurophysiol 1998;108:291–298.

44. Gharib S, Sutherling WW, Nakasato N, et al. MEG and ECoG localization accuracy test. Electroencephalogr Clin Neurophysiol 1995; 94:109–114.

45. Yoo SS, Talos IF, Golby AJ, Black PM, Panych LP. Evaluating requirements for spatial resolution of fMRI for neurosurgical planning. Hum Brain Mapp 2004;21:34–43.

46. Duong TQ, Kim DS, Ugurbil K, Kim SG. Localized cerebral blood flow response at submillimeter columnar resolution. Proc Natl Acad Sci U S A 2001;98:10904–10909.

47. Lu H, Golay X, Pekar JJ, Van Zijl PC. Functional magnetic resonance imaging based on changes in vascular space occupancy. Magn Reson Med 2003;50:263–274.

48. Gallen CC, Schwartz BJ, Bucholz RD, et al. Presurgical localization of functional cortex using magnetic source imaging. J Neurosurg 1995;82:988–994.

49. Schiffbauer H, Berger MS, Ferrari P, Freudenstein D, Rowley HA, Roberts TP. Preoperative magnetic source imaging for brain tumor surgery: a quantitative comparison with intraoperative sensory and motor mapping. J Neurosurg 2002;97:1333–1342.

50. Fink GR, Frackowiak RS, Pietrzyk U, Passingham RE. Multiple nonprimary motor areas in the human cortex. J Neurophysiol 1997;77:2164–2174.

51. Van Oostende S, Van Hecke P, Sunaert S, Nuttin B, Marchal G. FMRI studies of the supplementary motor area and the premotor cortex. Neuroimage 1997;6:181–190.

52. Ehrsson HH, Kuhtz-Buschbeck JP, Forssberg H. Brain regions controlling nonsynergistic versus synergistic movement of the digits: a functional magnetic resonance imaging study. J Neurosci 2002;22:5074–5080.

53. Yetkin FZ, Mueller WM, Morris GL, et al. Functional MR activation correlated with intraoperative cortical mapping. AJNR Am J Neuroradiol 1997;18:1311–1315.

54. Righini A, de Divitiis O, Prinster A, et al. Functional MRI: primary motor cortex localization in patients with brain tumors. J Comput Assist Tomogr 1996;20:702–708.

55. Schlosser R, Hunsche S, Gawehn J, et al. Characterization of BOLD-fMRI signal during a verbal fluency paradigm in patients with intracerebral tumors affecting the frontal lobe. Magn Reson Imaging 2002;20:7–16.

56. Roberts TP, Rowley HA. Mapping of the sensorimotor cortex: functional MR and magnetic source imaging. AJNR Am J Neuroradiol 1997;18:871–880.